Published in final edited form as:
J Org Chem. 2006 December 8; 71(25): 9261–9270. doi:10.1021/jo061235h.

Substituent Effects in C_6F_6-C_6H_5X Stacking Interactions

Benjamin W. Gung[a] and **Jay C. Amicangelo**[b]
Department of Chemistry & Biochemistry, Miami University, Oxford, Ohio 45056, gungbw@muohio.eduSchool of Science, Penn State Erie, The Behrend College, Erie, Pennsylvania 16563, jca11@psu.edu

Abstract

Parallel displaced and sandwich configurations of hexafluorobenzene-substituted benzene dimers are studied by ab initio molecular orbital methods up to the MP2(full)/aug-cc-pVDZ level of theory to reveal how substituents influence π-π interactions. Two minimum energy configurations are found, one with the substituent group away from (**2a–2f**) and the other with the substituent group on top of the π-face of the hexafluorobenzene (**3a–3f**). Higher binding energies are predicted for dimers with the substituent on the π-face (**3a–3f**). All sandwich dimers (**4a–4e**) are found to be saddle points on the potential energy surfaces. A parallel displaced minimum energy configuration is also predicted for the parent complex, C_6F_6-C_6H_6, which is in contrast to predictions based on quadrupole moments of benzene and hexafluorobenzene. The preference for the parallel displaced, rather than the sandwich configuration, is rationalized based on the smaller interplanar distance in the former. The closeness of contact in the parallel displaced dimers leads to greater binding energies. The shape of the electron density isosurface of the monomers is suggested to provide a guide for the prediction of how arenes stack with one another. A large difference in binding energy between the C_6F_6 complex of aniline (**3e**) and N,N-dimethylaniline (**3f**) is calculated and charge-transfer interactions are suggested to play a role in the latter.

Introduction

Weak noncovalent forces such as π-π stacking are important in biomolecular recognition and in crystal engineering.[1–6] π-π Stacking interactions also play a significant role in the outcomes of stereoselectivity in synthetic organic reactions.[7–10] Not surprisingly, there have been widespread interest in the magnitude and origin of π-π interactions.[2–5, 11–14] Recently we reported experimental studies aimed at an energetic quantification and an improved understanding of noncovalent interactions involving aromatic rings.[13, 14] Our experimental studies using triptycene derived models measure arene-arene interactions in the parallel displaced configuration. Opposite trends of substituent effects were observed for strongly perturbed vs. mildly perturbed arenes.[13] Furthermore, charge-transfer bands were observed in the interactions that involved perfluorinated arenes and an N,N-dimethylaminobenzyl group, which also exhibited greater than normal binding energy based on the Hammett plot.[13, 15] To better understand our experimental results and to examine the relative importance of electrostatic, dispersion, and charge-transfer interactions, we initiated a study of substituent effects in C_6F_6-C_6H_5X interactions by ab initio molecular orbital methods. Although computational studies of benzene dimers have been performed extensively,[16–22] studies of substituted benzene dimers are relatively limited.[11, 23, 24] Theoretical studies on C_6F_6-C_6H_6 interactions found that the edge-to-face or T-shaped configurations, with either a C–H bond pointed towards the C_6F_6 π cloud or a C–F bond pointed towards the C_6H_6 π cloud, were

[a]Miami University,
[b]The Behrend College

approximately 3–5 kcal/mol less stable than the sandwich and the parallel-displaced arrangements.[12, 25, 26] These results are consistent with experimental observations of equimolar mixture of hexafluorobenzene and benzene, which shows nearly parallel stacking configuration of C_6F_6-C_6H_6.[27, 28] To our knowledge theoretical studies of substituted benzene-hexafluorobenzene interactions have not been reported.

Stacking arrangements have been identified both in gas phase and in solid state studies of C_6F_6-C_6H_6 dimers.[28–30] The advantage of recognizing the role played by the quadrupole moments of benzene and hexafluorobenzene has been demonstrated convincingly.[31–33] Many have depicted these aromatic molecules topologically as a d_z2 orbital with opposite charges labeled for the center belt region and the top and bottom lobes.[2–4] It appears that the consideration of quadrupole moments provides an easy way to visualize the charge distribution of aromatics and correctly predicts the preferred geometry of π-π interactions. However, this study shows that the importance of the quadrupole moments may have been overemphasized and erroneous conclusions may be reached if one considers the electrostatic force alone. The implied conclusion from considering exclusively two opposite quadrupoles is that the face-to-face dimer of C_6F_6-C_6H_6 should be the energy minimum.[2–4] From the popular sketches of the quadrupole moments of benzene and hexafluorobenzene, the C_6F_6-C_6H_6 dimer has already been depicted as a representative of the sandwich configuration.[3] However, this and another recent study show that the sandwich configuration of the C_6F_6-C_6H_6 dimer is a saddle point, rather than an energy minimum.[12]

This study demonstrates that the magnitude of the attractive interactions of C_6F_6-C_6H_5X dimers depends on the closeness of contact between the arenes and on the donor ability of the benzene substituent (X). Similar to our experimental observations,[13] the results from this theoretical study are also consistent with an electron donor-acceptor relationship in addition to electrostatic considerations. The optimized minimum configurations of C_6F_6-C_6H_5X dimers have a parallel displaced, rather than a sandwich configuration, indicating more complex interactions are involved than a simple Coulombic attraction. Important factors such as dispersion and charge-transfer are demonstrated by considering the shape of the electron density surface and the Hammett free energy relationship.

Computational Methods

Theoretical calculations were carried out using the Gaussian 98 and 03 suite of programs.[34] All of the monomers were fully optimized at the MP2(full) level using Dunning's augmented correlation-consistent polarized valence triple-ζ basis set (aug-cc-pVTZ), except for the N,N-dimethylaniline monomer which was optimized using Dunning's correlation-consistent polarized valence triple-ζ basis set (cc-pVTZ).[35–37] Interaction energies were calculated for parallel-displaced dimers of hexafluorobenzene with several mono-substituted benzenes (C_6F_6-C_6H_5X) at the MP2(full) level using four different basis sets (6-31+G**, 6-311+G**, 6-311++G(2d,2p), and aug-cc-pVDZ).[35–37] The substituents in the mono-substituted benzenes are F, CN, CH_3, NH_2, and $N(CH_3)_2$. During the dimer energy calculations, the monomer geometries were not allowed to vary. However, for the dimers, the energies of the geometric configurations were examined for the parallel-displaced orientation and the intermonomer center of mass distances were varied to determine the largest interaction energy. Both the vertical, R_1, and the horizontal, R_2, center of mass distances were systematically varied starting from the values of 3.4 and 1.6 Å, respectively, which are the optimal values determined by Sherrill and co-workers for the parallel-displaced benzene dimer.[20, 38] R_2 values are denoted as positive for dimers (**2**) with the phenyl substituent away from the hexafluorobenzene face while denoted as negative for dimers (**3**) with the phenyl substituent on top of the hexafluorobenzene. Basis set superposition error (BSSE) was accounted for using the counterpoise correction method.[39, 40] Electrostatic potential surfaces of the aromatic rings

are generated by mapping the HF/6-31+G** electrostatic potentials onto surfaces of molecular electron density (isosurface of 0.0004 electrons au^{-3}) and color coding, using the program GaussView.[41] In all surfaces shown, the electrostatic potential values range from +0.04 to −0.04 hartree/mol (+25 kcal/mol to −25 kcal/mol), with red signifying a value greater than or equal to the maximum in negative potential and blue signifying a value greater than or equal to the maximum in positive potential.

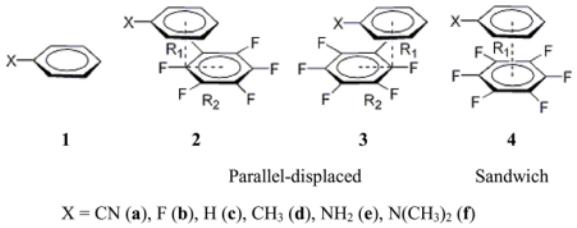

X = CN (**a**), F (**b**), H (**c**), CH_3 (**d**), NH_2 (**e**), $N(CH_3)_2$ (**f**)

Our primary interest in this study is in the relative energetics of the parallel displaced C_6F_6-C_6H_5X dimers and our choices of theoretical methods enabled us to perform calculations at a practical pace with our computational resources (average ~24 hr/structure). Several other studies have shown that in order to obtain accurate absolute interaction energies of π-π systems, very large basis sets, such as the aug-cc-pVTZ and the aug-cc-pVQZ basis sets, and electron correlation methods beyond MP2, such as the CCSD(T) method, are needed (which are beyond our computational resources).[11, 12, 23, 42] To assess whether the relative energies of the substituted complex C_6F_6-C_6H_5X remain relatively constant with different basis sets, we have performed calculations with four different basis sets at the MP2 (full) level of theory for both complex series **2** and **3**. A greater binding energy is found with a larger basis set. However, the relative energies do remain relatively constant. In general, all complexes have the same proportional increase in energy as basis set increases in size. For complex series (**2**), the relative strength of the complexes follows the same order according to substituents for all basis sets employed. For complex series (**3**) where the substituent X is on top of the C_6F_6 ring, all complexes follow the same relative energetic order except for complex **3a** (X = CN), which exhibits a slight disproportional increase in binding energy with a larger basis set. The results performed at the highest level of theory indicate a diminished difference in interaction energies between X = CN, F and H. This is consistent with our experimental observations.[13]

Computational Results

The interplanar (R_1) and the center of mass separation (R_2) of the parallel-displaced C_6F_6-C_6H_5X (X = H, F, CN, CH_3, NH_2, $N(CH_3)_2$) dimers were calculated at the MP2(full)/6-31 +G** level by systematically optimizing the R_1 and R_2 distances, with the starting values being 3.4 and 1.6 Å, respectively. The R_1 distance was optimized first using a fixed R_2 value of 1.6 Å and was varied from 2.9 to 3.6 Å. For all C_6F_6-C_6H_5X dimers, the optimal R_1 distance was determined to be 3.4 Å and the BSSE corrected interaction energies calculated using this R_1 value and R_2 = 1.6 Å are given in Table 1.

Using the optimized R_1 value of 3.4 Å, the R_2 values were varied from −2.0 to 2.0 Å and the BSSE corrected energy was calculated at each distance. Positive values of R_2 (**2**) indicate that the functional group is moving away from the center of the hexafluorobenzene ring and negative values of R_2 (**3**) indicate that the functional group is moving towards the center of the hexafluorobenzene ring. A distance of 0.0 Å is, therefore, for a sandwich complex (**4**). For positive R_2 distances, the optimal values were determined to be between 0.9 and 1.1 Å for all dimers and for negative R_2 distances the optimal values were determined to be between −0.8 and −1.3 Å for all dimers. The BSSE corrected interaction energies at the optimum positive and negative R_2 distances are listed in Table 2 at four different levels of theory. The optimized

structures are shown in Figures 1 and 2, respectively. As can be seen in Table 2, the magnitudes of the interaction energies at both the positive and negative R_2 distances are larger than the values at R_2 = 1.6 Å (Table 1). Comparing the interaction energies for a given dimer at the optimal positive and negative R_2 distances to each other, it can be seen that the energies for the negative R_2 distances are generally larger than those for positive R_2 values, indicating a significant interaction between the substituent X and the C_6F_6 ring. The general trend in the interaction energies for complex series **2** at the optimal R_1 distances is N,N-dimethylaniline > aniline > toluene > benzene > fluorobenzene > cyanobenzene, although the magnitudes of the N,N-dimethylaniline, aniline, and toluene dimers depend to a small extent on whether the lone pair or the hydrogen is pointing towards or away from the hexafluorobenzene ring. The general trend in the interaction energies for complex series **3** follows the same order except where X = CN. With the larger basis set aug-cc-pVDZ, complex **3a** (X = CN) exhibits a slightly larger interaction energy than complexes **3b** (X = F) and **3c** (X = H). This is consistent with our recent experimental observations and we will discuss further in later sections.

Sandwich C_6F_6-C_6H_5X Dimers (4a–e)

The BSSE corrected interaction energies of the sandwich C_6F_6-C_6H_5X (X = H, F, CN, CH_3, NH_2, $N(CH_3)_2$) dimers were calculated at the MP2(full)/6-31+G** level by systematically varying the interplanar distance from 3.0 to 4.0 Å. For all C_6F_6-C_6H_5X sandwich dimers, the optimal distance was determined to be either 3.5 or 3.6 Å and the interaction energies calculated at these distances are given in Table 3. The optimized sandwich structures are shown in Figure 3. Similar to the parallel-displaced C_6F_6-C_6H_5X dimers, the trend in the interaction energies for the sandwich dimers is predicted to be N,N-dimethylaniline > aniline > toluene > benzene > fluorobenzene > cyanobenzene. The sandwich dimers are determined to be saddle points and the parallel-displaced orientation is the minimum energy configuration for these complexes (see Figures 4 and 5).

Discussion

A. General Trend in Interaction Energies

In accordance with our recent experimental results,[13] both the parallel displaced and sandwich C_6F_6-C_6H_5X dimers are predicted to have the general trend that the electron-donating substituent enhances the interaction energies (Tables 1, 2, and 3). The overall order of interaction energies is found to be N,N-dimethylaniline > aniline > toluene > benzene > fluorobenzene > cyanobenzene in complex series **2**. This is in contrast to interactions between benzene-substituted benzenes, which exhibit the opposite trends, i.e., electron-withdrawing substituents lead to stronger binding energies.[11, 13, 14, 43] This reversal in trend is consistent with the opposite signs of the quadrupole moments of hexafluorobenzene and benzene, which suggests electrostatic forces play a prominent role in the interactions of the C_6F_6-C_6H_5X dimers, at least for the complex series **2**. However, this does not mean the interactions are entirely due to electrostatic forces. Consistent with Sherrill's results,[11] dispersion forces are found to be important and in addition, donor-acceptor interactions also play an important role as we will demonstrate.

The first indication of the importance of dispersion forces is the general stronger interactions displayed by complex series **3** than series **2**. The substituent X is in contact with the C_6F_6 ring in complex **3**, which increases the contact surface area between the two aromatic rings, a requirement for dispersion interactions. The second indication is the gradual leveling off and slight reversal of the substituent effect in complex series **3**. At the highest level of theory (MP2/aug-cc-pVDZ) performed in this study, the substituent effect in **3** is calculated as N,N-dimethylaniline > aniline > toluene > cyanobenzene > benzene ~ fluorobenzene. This is interesting in that the electrostatic potential is no longer the dominant factor when the

substituent is an electron-withdrawing group. Since a CN group has a larger surface area than a fluorine or a hydrogen atom, the results indicate the importance of dispersion forces. Our recent experimental results, which employs a model mimicking complex series **3**, have demonstrated that the interactions between a pentafluorobenzoate and a substituted benzyl group are attractive and the trend observed for enhancing attractive interactions was 4-N,N-dimethylanilinyl > 4-methoxyphenyl > 4-methylphenyl > phenyl ~ 4-fluorophenyl ~ 4-trifluoromethylphenyl.[13] Our experimental results showed that in the interactions with a strongly electron-deficient arene, electron-rich arenes gave rise to larger interaction energies while electron-poor arenes displayed similar interaction energies. Thus, the computational results agree with the experimental observations within system and experimental errors.

The plot in Figure 4 illustrates the dependence of interaction energy on the center of mass separation distance R_2 for the C_6F_6-C_6H_5CN dimer and is representative of the R_2 dependence for all dimers studied (see supporting information). Two types of minimum configurations (**2** and **3**) and a saddle point (**4**) are found for the stacking C_6F_6-C_6H_5X dimers. Stronger interaction energies are found for dimers **3a–3f** where the substituent X is in contact with the π-face of the C_6F_6 ring (see graphics in Figure 2). The energy difference between the two minimum configurations **2a–2f** and **3a–3f** depends on the substituent group. In other words, the energy difference between R_2 = positive and R_2 = negative are computed to be (kcal/mol): 0.82 (CN), 0.37 (F), 0.59 (CH_3), 0.99 (NH_2), and 1.41 ($N(CH_3)_2$) at the MP2/aug-cc-pVDZ level of theory. The most negative interactionenergy for each configuration was chosen to be compared in consideration of the lone pair inversion and methyl group rotation under normal conditions. The difference in contacting surface area between complex **2** and **3** seems to be consistent with the difference of the magnitude in interaction energies. For example, the difference between **2a** and **3a** (X = CN) in contacting surface area is greater than that between **2b** and **3b** (X = F) and the interaction energy difference follows the same order. The large preference displayed by the N,N-dimethylamino group suggests the involvement of charge-transfer interactions.

A finer structural difference of the dimers involves the relative orientation of the substituent group X. With symmetrical substituents such as CN and F (**a** and **b**), there is only one minimum configuration for either dimers **2a**–**c** or **3a**–**c** (Figure 1 & 2). However the magnitudes of the N,N-dimethylaniline, aniline, and toluene interaction energies with C_6F_6 depend to a small extent on whether the N,N-dimethylaniline and aniline lone pairs or the toluene methyl hydrogen are pointing at or away from the lower hexafluorobenzene ring (for example, see **3d**, **3d′** and **3e**, **3e′**). With the substituent *not* in contact with the π-face of C_6F_6 (**2a–2f**, Figure 1), there is essentially no difference for the toluene dimer (−6.12 kcal/mol, **2d** and −6.13 kcal/mol, **2d′**) whether the hydrogen is pointing at or away from the C_6F_6 ring. For the aniline (−6.34 kcal/mol, **2e** and −5.88 kcal/mol, **2e′**) and N,N-dimethylaniline (−7.05 kcal/mol, **2f** and −6.54 kcal/mol, **2f′**) dimers, the more stable configuration (**2e** and **2f**) is predicted when the lone pair is pointing away from the hexafluorobenzene ring. This is likely due to a repulsive interaction in **2e′** and **2f′** between the lone pair on nitrogen and a nearby fluorine atom from C_6F_6 when the lone pair is pointing at the hexafluorobenzene ring.

With the substituent *in* contact with the π-face of C_6F_6 (**3a–3f**, Figure 2), there are differences for the toluene, aniline, and N,N-dimethylaniline dimers (**3d–3f** and **3d′–3f′**) with regard to which direction the hydrogen or the lone pair is pointing. For the toluene-hexafluorobenzene dimer, the more stable configuration is predicted when the hydrogen atom is pointing away from the C_6F_6 ring (−6.45 kcal/mol, **3d**, vs. −5.55 for **3d′**, Figure 2). This is most likely due to a repulsive interaction between the methyl hydrogen atom and the nearest fluorine atom of the C_6F_6 ring in **3d′**. The distance between the hydrogen atom and the fluorine atom in contact in **3d** is 2.35 Å, which is shorter than the sum of the van der Waals radii for the two atoms in question.[44] For the complexes of aniline (−6.54 kcal/mol, **3e** and −7.30 kcal/mol, **3e′**) and

N,N-dimethylaniline (−8.41 kcal/mol, **3f′**), the more stable configuration (**3e′** and **3f′**) is predicted when the lone pair is pointing at the hexafluorobenzene ring. When the lone pair is pointing away, the potential energy surface is flat for N′N-dimethylaniline complex and no minimum energy conformation corresponding to **3f** was located. The preference for the nitrogen lone pair to point at the C_6F_6 ring is likely due to a combination of electrostatic, charge-transfer, and dispersion effects. More discussion on the origin of the enhanced attraction when R_2 = negative will be presented later.

B. Closeness of Contact and the Minimum Stacking Configuration

By definition set forth in this study, when the center of mass separation R_2 = 0.0 Å, the dimer assumes the sandwich configuration. The sandwich configuration is computed to be a saddle point, rather than a minimum along the parallel displaced coordinate and this saddle point exists even for the symmetrical dimer C_6F_6-C_6H_6 (Figure 5). The energy barriers along this coordinate generally range from 0.62 kcal/mol for the C_6F_6-C_6H_6 dimer to 1.98 kcal/mol for the C_6F_6-$C_6H_5N(CH_3)_2$ dimer. At the sandwich configuration, mimina are found along the symmetrical coordinate (R in Table 3) at slightly larger distances (3.5–3.6 Å) and the energy differences between the parallel displaced minima and the sandwich minima range from 0.27 kcal/mol for the C_6F_6-C_6H_6 dimer to 1.50 kcal/mol for the C_6F_6-$C_6H_5N(CH_3)_2$ dimer.

As described earlier, the C_6F_6-C_6H_6 dimer has been depicted in the literature as a representative of a face-to-face aromatic dimer. The face-to-face graphical depiction suggests that the interactions between hexafluorobenzene and benzene are dominated by electrostatic attractions. However the fact that the sandwich configuration is not the energy minimum is at odds with this simple picture. As pointed out by both Reisse and Dougherty, the representation of the electronic distribution of a molecule as a multipole expansion is valid only at large interaction distances.[32, 33] Because of the distance requirement, the cation-π interaction cannot be quantitatively modeled as just an ion-quadrupole interaction when van der Waals contact distance is involved.[33] For the same reason, neither can the benzene-hexafluorobenzene interaction be quantitatively modeled as just a quadrupole-quadrupole interaction. The argument should be even more important here since there are two quadrupoles involved. In C_6F_6-C_6H_6 stacking interactions, the dimensions of the quadrupole (e.g., the distance between the two centers of negative charge in hexafluorobenzene) are greater than the separation distance between the arenes. It is clearly inappropriate to make any quantitative argument based on a multipole expansion. Similar to cation-π interactions,[45] the structures of hexafluorobenzene and benzene dimer cannot be rationalized unless other terms such as dispersion and charge-transfer are also considered. In other words, the interactions between hexafluorobenzene and benzene cannot be treated as two simple quadrupoles with opposite signs.

Theoretical studies from this work and others are consistent with experimental observationsconcerning the C_6F_6-C_6H_6 dimer.[12, 25, 26] A low temperature crystal structure of an equimolar mixture of hexafluorobenzene and benzene shows that nearly parallel molecules stack alternately in infinite columns with an interplanar distance of about 3.4 Å and an intercentroid distance of 3.7 Å.[28] The difference between the interplanar and intercentroid distances clearly shows a parallel displaced structure.

The optimized interplanar distance between hexafluorobenzene and benzene in a sandwich configuration is 3.6 Å (Figure 3). This distance is decreased to 3.4 Å when the center of mass separation (R_2) is allowed to change from 0.0 to 1.0 Å (Figure 1 and 5). When the interplanar distance is fixed at 3.4 Å and R_2 is allowed to change between −2.0 and 2.0 Å, a saddle point appears at R_2 = 0.0 Å, (Figure 5). The sandwich configuration does not allow as close contact between the two arenes as the parallel-displaced configuration. An examination of the electron

density isosurface of hexafluorobenzene and benzene prompts us to suggest a new application of the 3D pictures for the understanding of the slightly displaced (−1.0 Å) dimer configuration.

Electrostatic potential surfaces of the aromatic monomers were generated by mapping the electrostatic potential onto the surfaces of the total electron density isosurface (0.0004 electrons au^{-3}) for each monomer using the program GaussView and are shown in Figure 6.[41] Dougherty has shown that electrostatic potential surfaces of aromatic compounds can serve as a useful qualitative guide in the prediction of cation-π interaction strengths.[46] It is shown here that the increasing negative electrostatic potential (more red) on the substituted benzenes also follows qualitatively the order of increasing strength for the C_6F_6-C_6H_5X dimers. A proposal to use the shape of the electron density surface to understand the preferred minimum energy configuration is presented.

We propose to use the shape and boundaries of the 3D molecular surface to predict arene-arene stacking arrangement. First, we will use the arene electron density surface to understand why the perfectly symmetrical sandwich configuration is not an energy minimum even for the C_6F_6-C_6H_6 dimer. As expected, the total electron density isosurfaces reveal that the aromatic π system has a doughnut-shaped surface, Figure 7 (a) and (b).

The six aromatic ring carbon atoms, which provide their p orbitals to make up the circular π system, are directly under the torus π orbital. In a sandwich configuration, the carbon atoms and hence theridge of the circular π system from one arene are directly on top of those from the other arene. The arenes are prevented form getting any closer than their density surfaces allow in the sandwich configuration by avoiding electrons from non-bonded atoms to occupy the same space. The interactions would becomesharply repulsive if electrons of the same spin from non-bonded atoms were to occupy the same space (steric effect). Thus the steric repulsion from the circular π system in the sandwich configuration causes the arenes to be separated at a greater distance (R = 3.6 Å). In the center of the circular π system, a bowl-shaped empty space is present in benzene and an even deeper void is present in hexafluorobenzene. As shown in Figure 7 (d), the arenes can achieve a closer contact distance by sliding away slightly from the sandwich configuration so that the empty space in the center of the circular π system of one arene is on top of a carbon atom from the other arene. By avoiding the direct contact of the ridges from the two π systems, a shorter vertical separation distance between the two arenes is achieved (3.3–3.4 Å vs. 3.5–3.6 Å for the sandwich configuration), which allows a better mesh of more atoms at their optimal van der Waals distances.

The closeness of contact of electron density surfaces between the arenes can also be seen from thepositions of the fluorine atoms relative to the benzene ring. The fluorine atoms have distinct spherical surfaces and by situating between two hydrogen atoms of the benzene ring, rather than on top of them, maximum contact of the surface area is achieved. Since dispersion forces are proportional to contacting surface area,[47] a greater contact leads to a greater stability. The parallel displaced configuration was also found to be more stable by Tsuzuki.[12] He showed that both the sandwich and the parallel displaced configuration are stabilized by electrostatic and dispersion forces. We propose here that by matching the empty space in the circular π system of one arene with a carbon atom from the other arene, a smaller interplanar separation is achieved, which allows a greater contact area and hence a greater stabilization from dispersion interactions. A smaller interplanar separation would also allow charge-transfer interactions to occur. In the case of C_6F_6-$C_6H_5N(CH_3)_2$ dimer, the next section argues for a case of charge-transfer interactions.

Stacking interactions play an important role in the stabilization of DNA structures.[47] The base pairs in double helical DNA structures arrange like a spiral stair case stacking on top of one another in a parallel displaced fashion. No sandwich stacking of any aromatic residues exists

in natural protein structures.[48, 49] The known structures of stacked octafluoronaphthalene with arenes and the bifunctional hexafluorophenyl phenylbutadiyne also show structure motifs that are remarkably similar to the feature described above for C_6F_6-C_6H_6.[2, 4, 6] These facts are consistent with our analysis using the electron-density isosurface of the arenes to achieve a maximum closeness of contact.

C. A Threshold for Charge-Transfer Interactions

A monotonic relationship between the binding energy and the Hammett constants has been interpreted to indicate a polar/π (or electrostatic) interaction between the arenes.[43] Hunter and coworkers have also used Hammett plots to illustrate the dominance of electrostatic forces in aromatic interactions.[50, 51] Although the Hammett constants do not necessarily correlate with ground state arene π–electron density,[11, 46] it does give some information about possible correlations between the calculated binding energies ($-\Delta E_{int}$) and classical substituent effects. The calculated binding energies vs. the Hammett σ_{para} constants are plotted in Figure 8 for complex series **2** C_6F_6-C_6H_5X (♦). Again the values with the largest magnitude are chosen for all complexes. This plot looks remarkably like the published results from ourrecent experimental studies conducted in $CDCl_3$ less the aniline complex.[13] Namely, the binding energy of the complex of C_6F_6-$C_6H_5N(CH_3)_2$ is much higher than that expected from the substituent constant.

Almost 40 years ago, charge-transfer bands were observed for 1:1 complexes of C_6F_6 and N.N-dimethylaniline, and N,N-dimethyltoludine, and N,N-diethylaniline.[52] No charge-transfer complex has been reported for aniline-hexafluorobenzene.[53] A charge-transfer band was observed for the model compound that we used to study the interaction between C_6F_6 and $C_6H_5N(CH_3)_2$.[13] The large difference in binding energy between **3e** and **3f** is likely due to the difference in the ionization potentials of aniline (7.7 eV) and N,N-dimethylaniline (7.1 eV).[54, 55] By examining the structures of **3e** and **3f** (Figure 2), CH-F hydrogen bonding in **3f** should be negligible. The distance between the nearest hydrogen atom of N,N-dimethylaniline and the fluorine atom in hexafluorobenzene is 3.2 Å while possible CH-F hydrogen bonds are reported anywhere between 2.36 Å and 2.86 Å.[44] Thus the relatively "normal" position of aniline complex (**3e**) on the Hammett plot is most likely due to the relatively higher ionization potential of aniline, therefore, lack of charge transfer interactions. Since the contributions from electrostatic and dispersive effects should be comparable for aniline and N,N-dimethylaniline, we attribute the higher binding energy of **3f′** to charge-transfer interactions arising from the lower ionization potential of N,N-dimethylaniline. The evidences that support this proposal include the observation of charge transfer bands for the complexes involving hexafluorobenzene and N,N-dimethylaniline,[52] our recent experimental results,[13] and this theoretical study. Since aniline does not seem to, but N,N-dimethylaniline does show a charge transfer interaction with hexafluorobenzene, it seems reasonable to suggest a threshold for charge-transfer interactions between arenes with different characteristics. The intensity of charge transfer interactions is inversely proportional to the difference between the ionization potential (IP) of the donor and the electron affinity (EA) of the acceptor.[56] The electron affinity of hexafluorobenzene is relatively small (0.53 eV) compared to typical π-acceptors such as *p*-benzoquinone (1.9 eV), chloranil (2.54 eV), and TCNE (3.17 eV), which explains why a strong donor is required to form a charge transfer complex with C_6F_6.

D. Distance Dependence of Interaction Energy at Short Contacting Range

Plot of interaction energy (MP2(full)/6-31+G**) vs. interplanar distance (R_1) for complexes C_6F_6-C_6H_5CN (▪), C_6F_6-C_6H_6 (●), and C_6F_6-$C_6H_5N(CH_3)_2$ (▲) are shown in Figure 9. The interaction energy of C_6F_6-$C_6H_5N(CH_3)_2$ is more than 3 kcal/mol larger than the other two complexes at R_1 = 3.3 Å, but levels off to less than 1 kcal/mol when $R_1 \geq 4$ Å. Assuming electrostatic and dispersion forces play major roles in these dimers, and in light of the evidence

presented in the previous section, we hypothesize that the exceedingly high attraction of C_6F_6-$C_6H_5N(CH_3)_2$ at close distance is due to the presence of charge-transfer interactions. To assess this hypothesis, we examined several model potential energy curves.

Assuming the interactions between C_6F_6 and C_6H_6 are limited to electrostatic and dispersionforces, we start with a simple Lennard-Jones (12-6) type potential function,[57] eq. (1), where E(r) is the distance dependent potential energy, r is the interplanar distance and a and b are adjustable constants.

$$E(r)=a/r^{12}+b/r^{6} \quad (1)$$

The two parameters (a and b) in eq. (1) were varied until a curve was obtained in which the minimum was at 3.4 Å and the potential energy was close to −5.43 kcal/mol, which is the interaction energy for the C_6F_6-C_6H_6 dimer at the MP2(full)/6-31+G** level. This was found to be when $a = 1.33 \times 10^7$ and $b = -1.70 \times 10^4$ and is represented as the solid blue curve in Figure 10. To model the distance dependence of the charge-transfer interaction, we use an inverse exponential function ($e^{-2r/L}$, where L is the sum of the van der Waals radii of the donor and acceptor) proposed by Dexter to model the distance dependence of the rate constant for excited state energy transfer via an electron transfer mechanism.[58, 59] In the current model, we use a value of L = 3.50 Å, which is the sum of the van der Waals radii of two carbon atoms. With the inclusion of this charge transfer term, the overall potential function is represented by eq. (2), where a,b, and c are adjustable constants, L is the van der Waals contact distance between the two arenes.

$$E(r)=a/r^{12}+b/r^{6}+c/e^{(-2r/L)} \quad (2)$$

Thus the new functional model includes a term for charge-transfer interaction in addition to the repulsive and the London force terms in the Lennard-Jones equation.

Two different constraints for the parameter c led to two plots and both are shown in Figure 10. The first was to adjust the value of c until the difference between the simple Lennard-Jones potential and the modified functional curve at 6.0 Å is equal to 0.45 kcal/mol, which is the calculated energy difference between the C_6F_6-$C_6H_5N(CH_3)_2$ and C_6F_6-C_6H_6 dimers at 6.0 A. This gives a value of c = −13.9 and is given as the dashed red curve in Figure 10. At 3.4 Å, this gives a difference of 2.0 kcal/mol between the simple Lennard-Jones potential and the modified functional curve. As a reminder, the MP2(full)/6-31+G** energy difference at 3.4 Å for the C_6F_6-$C_6H_5N(CH_3)_2$ and C_6F_6-C_6H_6 dimers is 2.98 kcal/mol. Therefore the energy difference at the minima between the two initial models is slightly lower than the calculated value, however, the relative shape of the model potential curves are similar to the calculated R_1 dependences shown in Figure 9. The next constraint was to adjust the c value until the difference between the simple Lennard-Jones potential and the modified functional curves at 10.0 Å is equal to 0.1 kcal/mol, which is the calculated energy difference between the C_6F_6-$C_6H_5N(CH_3)_2$ and C_6F_6-C_6H_6 dimers at 10.0 Å. This gives a value of c = −30.0 and is given as the dashed green curve in Figure 10. At 3.4 Å, this gives a difference of 4.3 kcal/mol between the simple Lennard-Jones potential and the modified functional curves. This is now slightly larger than the calculated difference of 2.98 kcal/mol, but again the relative shapes of the model potential curves are similar to the calculated R_1 dependences shown in Figure 9. These models suggest that the addition of a charge transfer interaction has the effect of increasing the strength of the interaction energy (lowering the well depth) when compared to a simple Lennard-Jones potential. These plots and the Hammett plot for the calculated binding energies are both consistent with our previous experimental studies in $CDCl_3$ and lend support for the hypothesis that a charge transfer interaction contributes to the unusually strong interaction energy of the N,N-dimethylaniline-hexafluorobenzene dimer.[13]

Conclusions

Perfluoroarene interactions have a rich history in both bioorganic chemistry and crystal engineering.[6, 60] A better understanding of the substituent effects in perfluoroarene interactions will help the rational design efforts in these areas. Three dimensional molecular electron density surfaces are calculated at the HF/6-31+G** level of theory. The calculated molecular shapes are proposed to be useful in predicting the stacking arrangement of perfluoroarenes. The proposal involves the staggering of the two arenes to avoid a head on overlap of the π systems. Interaction energies for the parallel displaced and sandwich C_6F_6-C_6H_5X dimers were calculated up to the MP2/aug-cc-pVDZ level of theory. Electron donating groups increase and electron-withdrawing groups decrease the interaction energies. N,N-dimethylamino group has by far the largest effect, increasing the interaction energy by nearly 3 kcal/mol relative to the unsubstituted benzene-hexafluorobenzene dimer. This substituent is even capable ofincreasing the interaction energy by one kcal/mol more than the amino group itself, despite the latter has a stronger electron-donating effect according the classical Hammett constant.[15] This anomaly is attributed to a charge-transfer effect for the N,N-dimethylamino complex, which is consistent with our previous experimental results.[13]

Supplementary Material

Refer to Web version on PubMed Central for supplementary material.

Acknowledgements

Acknowledgment is made to the donors of the Petroleum Research Fund (PRF#40361-AC1) administered by the American Chemical Society. BWG is grateful for support from the National Institutes of Health (GM069441). JCA acknowledges Penn State Erie, The Behrend College for the funds to purchase the Gaussian and GaussView software and Jennifer Holt for the use of an additional computer to run some of the larger basis set calculations.

References

1. Kool ET, Morales JC, Guckian KM. Angew Chem-Int Edit 2000;39(6):990–1009.
2. Hunter CA, Lawson KR, Perkins J, Urch CJ. J Chem Soc-Perkin Trans 2 2001;(5):651–669.
3. Waters ML. Curr Opin Chem Biol 2002;6(6):736–741. [PubMed: 12470725]
4. Meyer EA, Castellano RK, Diederich F. Angew Chem-Int Edit 2003;42(11):1210–1250.
5. Sarkhel S, Rich A, Egli M. J Am Chem Soc 2003;125(30):8998–8999. [PubMed: 15369340]
6. Coates GW, Dunn AR, Henling LM, Dougherty DA, Grubbs RH. Angewandte Chemie, International Edition in English 1997;36(3):248–251.
7. Corey EJ, Loh TP, Roper TD, Azimioara MD, Noe MC. J Am Chem Soc 1992;114(21):8290–8292.
8. Ishihara K, Gao QZ, Yamamoto H. J Am Chem Soc 1993;115(22):10412–10413.
9. Jones GB. Tetrahedron 2001;57(38):7999–8016.
10. Jones GB, Chapman BJ. Synthesis-Stuttgart 1995;(5):475–497.
11. Sinnokrot MO, Sherrill CD. J Am Chem Soc 2004;126(24):7690–7697. [PubMed: 15198617]
12. Tsuzuki S, Uchimaru T, Mikami M. J Phys Chem A 2006;110(5):2027–2033. [PubMed: 16451038]
13. Gung BW, Patel M, Xue XW. J Org Chem 2005;70(25):10532–10537. [PubMed: 16323868]
14. Gung BW, Xue XW, Reich HJ. J Org Chem 2005;70(9):3641–3644. [PubMed: 15845001]
15. Isaacs, N. Physical Organic Chemistry. 2. Longman; New York: 1995. p. 877
16. Jorgensen WL, Severance DL. J Am Chem Soc 1990;112(12):4768–4774.
17. Jaffe RL, Smith GD. J Chem Phys 1996;105(7):2780–2788.
18. Hobza P, Selzle HL, Schlag EW. J Phys Chem 1996;100(48):18790–18794.
19. Tran F, Weber J, Wesolowski TA. Helv Chim Acta 2001;84(6):1489–1503.
20. Sinnokrot MO, Valeev EF, Sherrill CD. J Am Chem Soc 2002;124(36):10887–10893. [PubMed: 12207544]

21. Tsuzuki S, Honda K, Uchimaru T, Mikami M, Tanabe K. J Am Chem Soc 2002;124(1):104–112. [PubMed: 11772067]
22. Zhao Y, Truhlar DG. J Phys Chem A 2005;109(19):4209–4212. [PubMed: 16833747]
23. Lee EC, Hong BH, Lee JY, Kim JC, Kim D, Kim Y, Tarakeshwar P, Kim KS. J Am Chem Soc 2005;127(12):4530–4537. [PubMed: 15783237]
24. Manojkumar TK, Kim D, Kim KS. J Chem Phys 2005;122(1)
25. HernandezTrujillo J, Colmenares F, Cuevas G, Costas M. Chem Phys Lett 1997;265(3–5):503–507.
26. Vanspeybrouck W, Herrebout WA, van der Veken BJ, Lundell J, Perutz RN. J Phys Chem B 2003;107 (50):13855–13861.
27. Overell JSW, Pawley GS. Acta Crystallographica Section B-Structural Science 1982 JUL;38:1966–1972.
28. Williams JH, Cockcroft JK, Fitch AN. Angew Chem-Int Edit Engl 1992;31(12):1655–1657.
29. Patrick CR, Prosser GS. Nature (London, United Kingdom) 1960;187:1021.
30. Steed JM, Dixon TA, Klemperer W. J Chem Phys 1979;70(11):4940–6.
31. Williams JH. Accounts Chem Res 1993;26(11):593–598.
32. Luhmer M, Bartik K, Dejaegere A, Bovy P, Reisse J. Bulletin De La Societe Chimique De France 1994;131(5):603–606.
33. Ma JC, Dougherty DA. Chem Rev 1997;97(5):1303–1324. [PubMed: 11851453]
34. Frisch, MJ.; Trucks, GW.; Schlegel, HB.; Scuseria, GE.; Robb, MA.; Cheeseman, JR.; Zakrzewski, VG.; Montgomery, JA.; Stratmann, RE.; Burant, JC.; Dapprich, S.; Millam, JM.; Daniels, AD.; Kundin, KN.; Strain, MC.; Farkas, O.; Tomasi, J.; Barone, V.; Cossi, M.; Cammi, R.; Mennucci, B.; Pomelli, C.; Adamo, C.; Clifford, S.; Ochterski, J.; Petersson, GA.; Ayala, PY.; Cui, Q.; Morokuma, K.; Malick, DK.; Rabuck, AD.; Raghavachari, K.; Foresman, JB.; Cioslowski, J.; Ortiz, JV.; Stefanov, BB.; Liu, G.; Liashenko, A.; Piskorz, P.; Komaromi, I.; Gomperts, R.; Martin, RL.; Fox, DJ.; Keith, T.; Al-Laham, MA.; Peng, CY.; Nanayakkara, A.; Gonzalez, C.; Challacombe, M.; Gill, PMW.; Johnson, B.; Chen, W.; Wong, MW.; Andres, JL.; Gonzalez, C.; Head-Gordon, M.; Replogle, ES.; Pople, JA. Gaussian 98. Gaussian Inc; Pittsburgh, PA: 1998.
35. Dunning TH. J Chem Phys 1989;90(2):1007–1023.
36. Kendall RA, Dunning TH, Harrison RJ. J Chem Phys 1992;96(9):6796–6806.
37. Woon DE, Dunning TH. J Chem Phys 1993;98(2):1358–1371.
38. Sinnokrot MO, Sherrill CD. J Phys Chem A 2004;108(46):10200–10207.
39. Boys SF, Bernardi R. Mol Phys 1970;19:553.
40. Vanduijneveldt FB, Vanduijneveldtvanderijdt J, Vanlenthe JH. Chem Rev 1994;94(7):1873–1885.
41. Frisch, A.; Dennington, RD.; Keith, TA. GaussView. 3. Gaussian, Inc; 2003.
42. Moran D, Simmonett AC, Leach FE, Allen WD, Schleyer PVR, Schaefer HF. J Am Chem Soc 2006;128(29):9342–9343. [PubMed: 16848464]
43. Cozzi F, Cinquini M, Annunziata R, Dwyer T, Siegel JS. J Am Chem Soc 1992;114(14):5729–5733.
44. Thalladi VR, Weiss HC, Blaser D, Boese R, Nangia A, Desiraju GR. J Am Chem Soc 1998;120(34): 8702–8710.
45. Dougherty DA. Science 1996;271(5246):163–168. [PubMed: 8539615]
46. Mecozzi S, West AP, Dougherty DA. Proc Natl Acad Sci U S A 1996;93(20):10566–10571. [PubMed: 8855218]
47. Guckian KM, Schweitzer BA, Ren RXF, Sheils CJ, Tahmassebi DC, Kool ET. J Am Chem Soc 2000;122(10):2213–2222.
48. Burley SK, Petsko GA. Science 1985;229(4708):23–28. [PubMed: 3892686]
49. McGaughey GB, Gagne M, Rappe AK. J Biol Chem 1998;273(25):15458–15463. [PubMed: 9624131]
50. Carver FJ, Hunter CA, Livingstone DJ, McCabe JF, Seward EM. Chem-Eur J 2002;8(13):2848–2859.
51. Cockroft SL, Hunter CA, Lawson KR, Perkins J, Urch CJ. J Am Chem Soc 2005;127(24):8594–8595. [PubMed: 15954755]
52. Beaumont TG, Davis KMC. Nature (London, United Kingdom) 1968;218(5144):865.
53. Foster, R. Organic Charge-Transfer Complexes. 1. Academic Press; New York: 1969. p. 470

54. Lias SG, Jackson JAA, Argentar H, Liebman JF. J Org Chem 1985;50(3):333–8.
55. Wu RH, Lin JL, Lin J, Yang SC, Tzeng WB. J Chem Phys 2003;118(11):4929–4937.
56. Mulliken, RS.; Person, WB. Molecular complexes; a lecture and reprint volume. Wiley-Interscience; New York: 1969.
57. Hirschfelder JO, Curtiss CF, Bird RB. 1954:22–35.
58. Dexter DL. J Chem Phys 1953;21:836.
59. Turro, NJ. Modern Molecular Photochemistry. University Science Books: Sausalito; California: 1991. p. 305-309.
60. Ohagan D, Rzepa HS. Chem Commun 1997;(7):645–652.

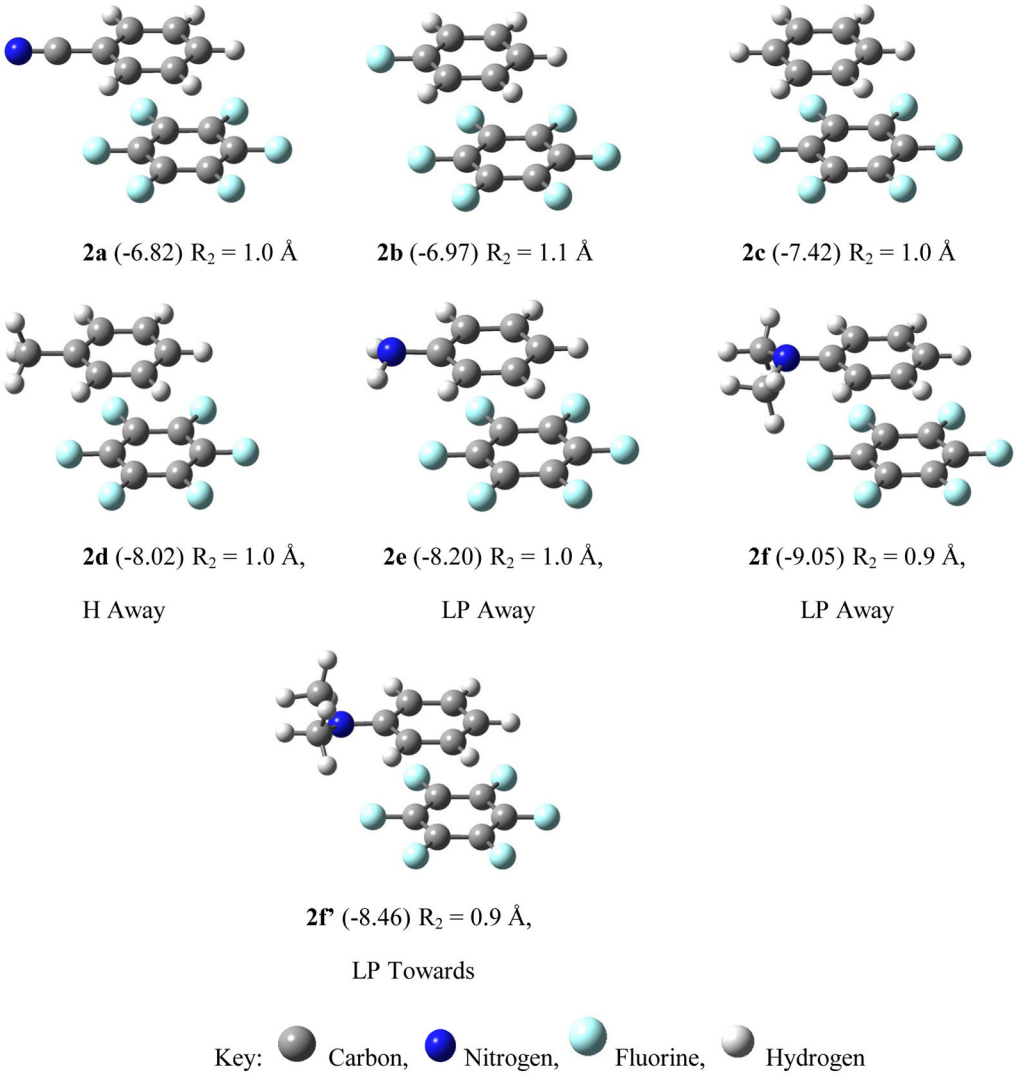

Figure 1.

Dimers (**2a**–**f**) for C_6F_6-C_6H_5X with the substituent slipping away from C_6F_6. R_1 = 3.4 Å and optimized R_2 (0.9–1.1 Å). The calculated MP2(full)/aug-cc-pVDZ interaction energies are listed in parentheses (kcal/mol).

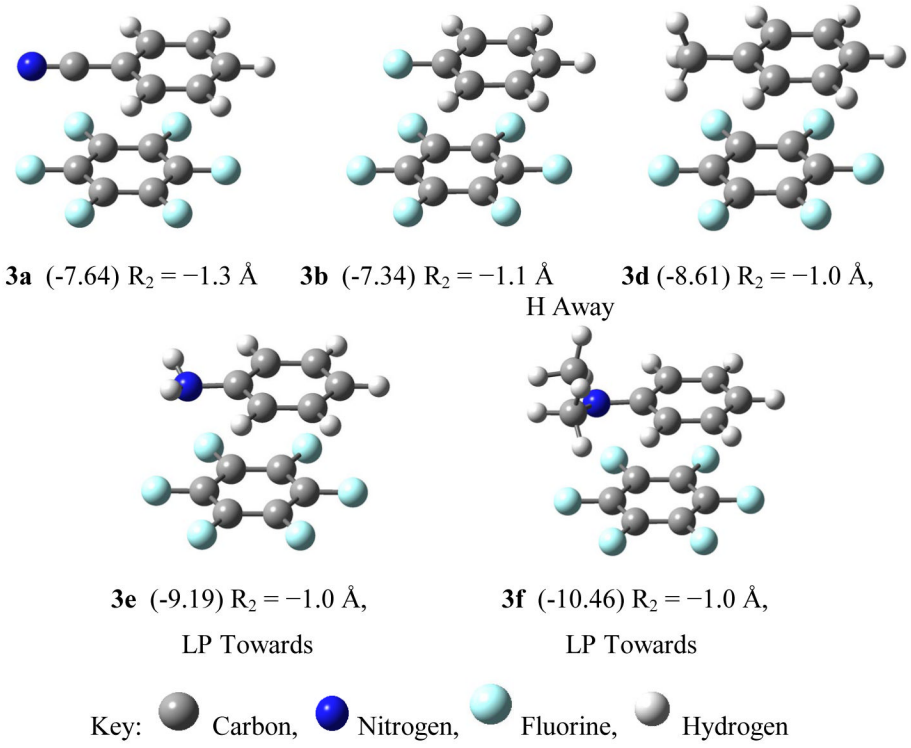

Figure 2.

Dimers (**3a**–**f**) for C_6F_6-C_6H_5X with the substituent slipping onto the C_6F_6 ring. Fixed R_1 = 3.4 Å and optimized R_2 (−0.8 to −1.3 Å). The calculated MP2(full)/aug-cc-pVDZ interaction energies are in parentheses (kcal/mol).

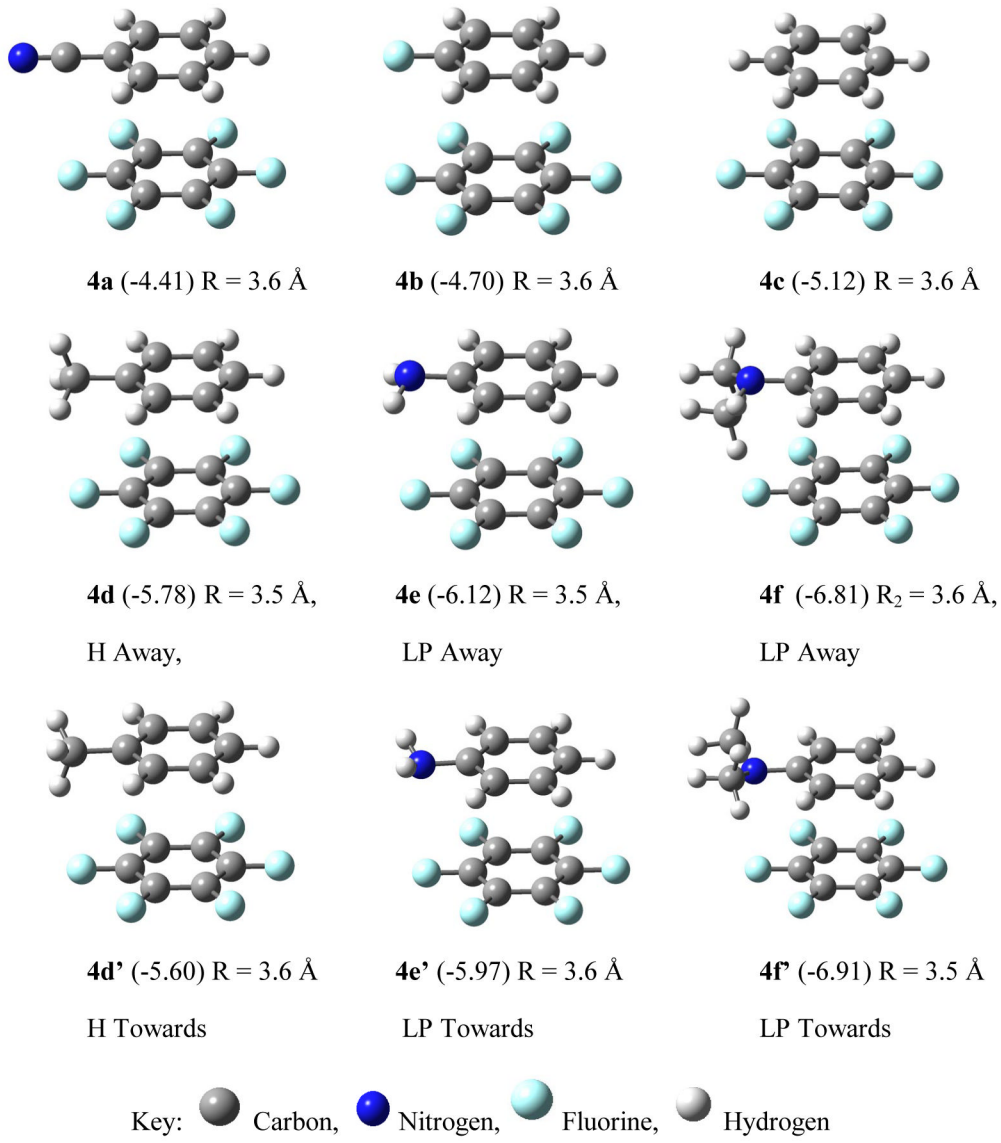

Figure 3.

Sandwich dimers (**4a**–**f**) of C_6F_6-C_6H_5X with optimized vertical separation distance (R = 3.5–3.6 Å). The calculated MP2(full)/6-31+G** interaction energies are listed in parentheses (kcal/mol).

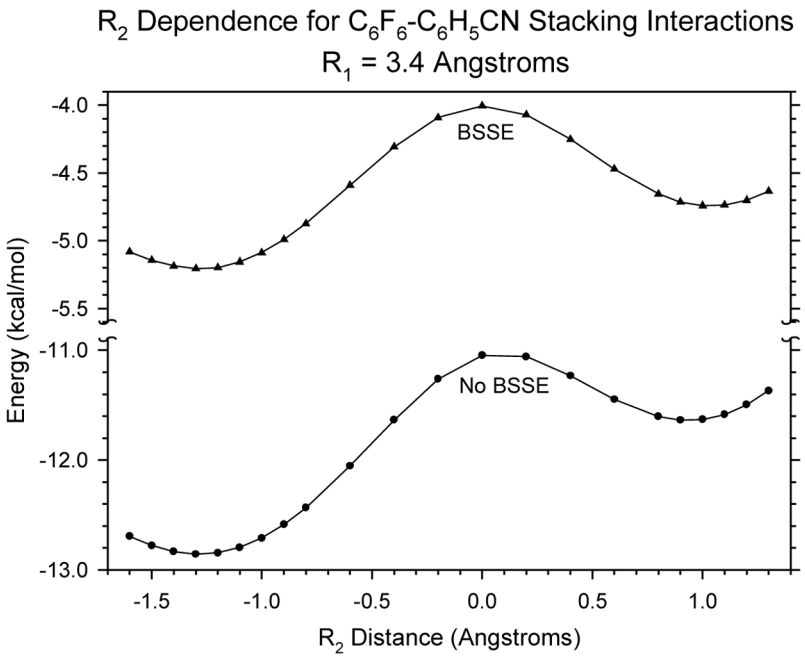

Figure 4.

Plot of interaction energy (MP2(full)/6-31+G**) vs. center of mass separation distance (R_2) for C_6F_6-C_6H_5CN. Top: with BSSE correction; bottom: without BSSE correction. Complex **2a** is located at the minimum position on the right with positive R_2 and complex **3a** is located at the minimum position on the left with negative R_2. Sandwich **4a** is located at the saddle point where R_2 = 0.0 Å.

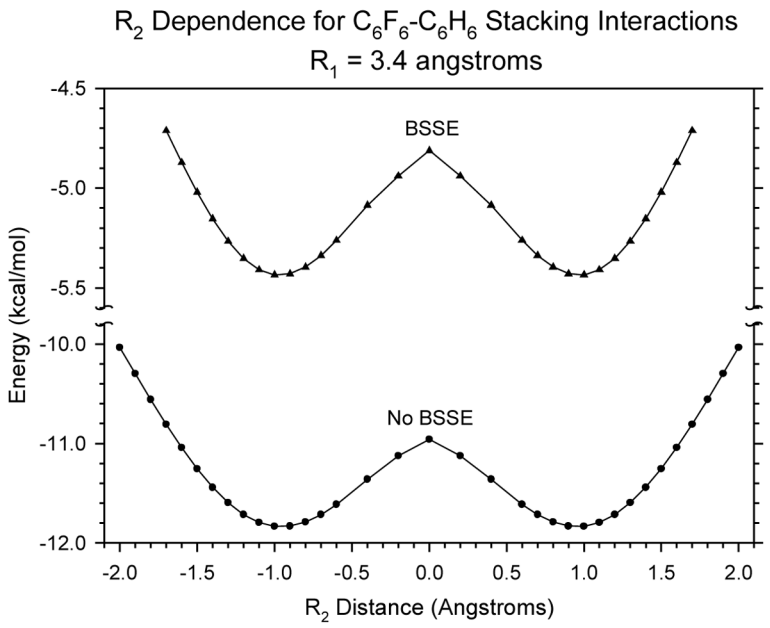

Figure 5.

Plot of interaction energy (MP2(full)/6-31+G**) vs. center of mass separation distance (R_2) for C_6F_6-C_6H_6. The sandwich configuration is at the saddle point where R_2 = 0.0 Å. Top: with BSSE correction; bottom: without BSSE correction.

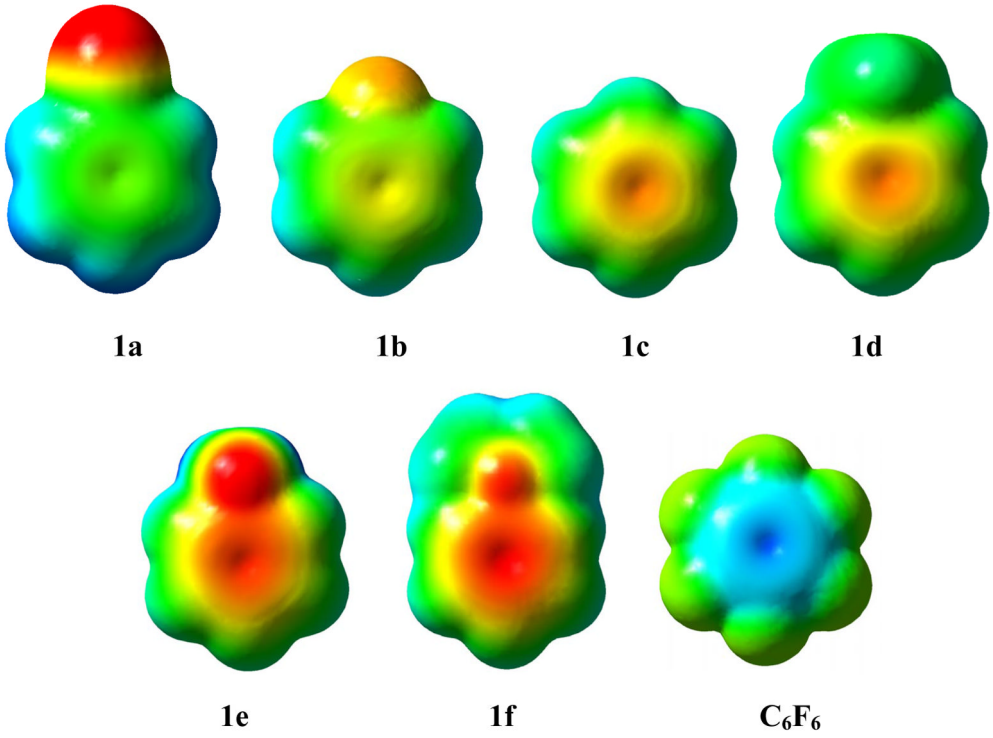

Figure 6.
Calculated HF/6-31+G** electrostatic potential surfaces of substituted benzenes (**1a–1f**) and hexafluorobenzene. From left to right: first row: C_6H_5CN, C_6H_5F, C_6H_6, $C_6H_5CH_3$, 2nd row: $C_6H_5NH_2$, $C_6H_5N(CH_3)_2$, and hexafluorobenzene.

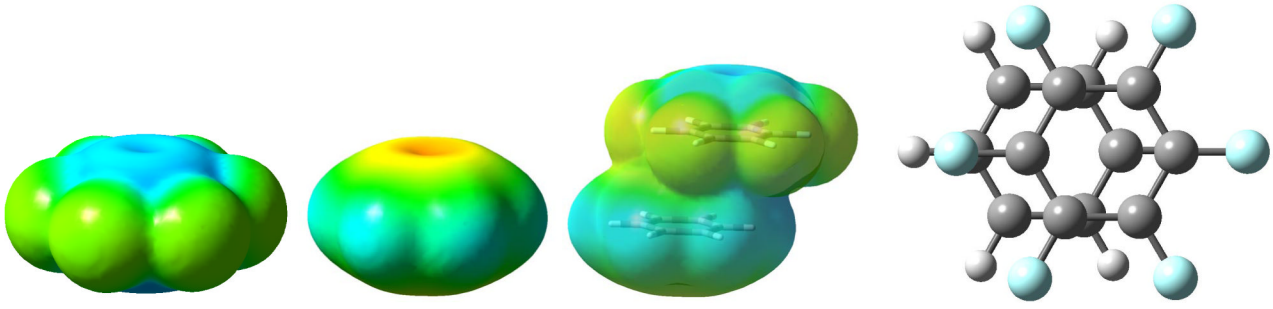

(a) C_6F_6 (b) C_6H_6 (c) C_6F_6-C_6H_6 (d) C_6F_6-C_6H_6

Figure 7.

(a), (b), and (c) ab initio electron density (HF/6-31+G**) isosurfaces color-mapped with electrostatic potential for C_6F_6, C_6H_6 and their complex. The isosurfaces show circular π systems with bowl-shaped centers. (d) Ball & Stick models for the optimized C_6F_6-C_6H_6 complex. A carbon atom from each arene is located near the center of the other arene to achieve a shorter vertical separation.

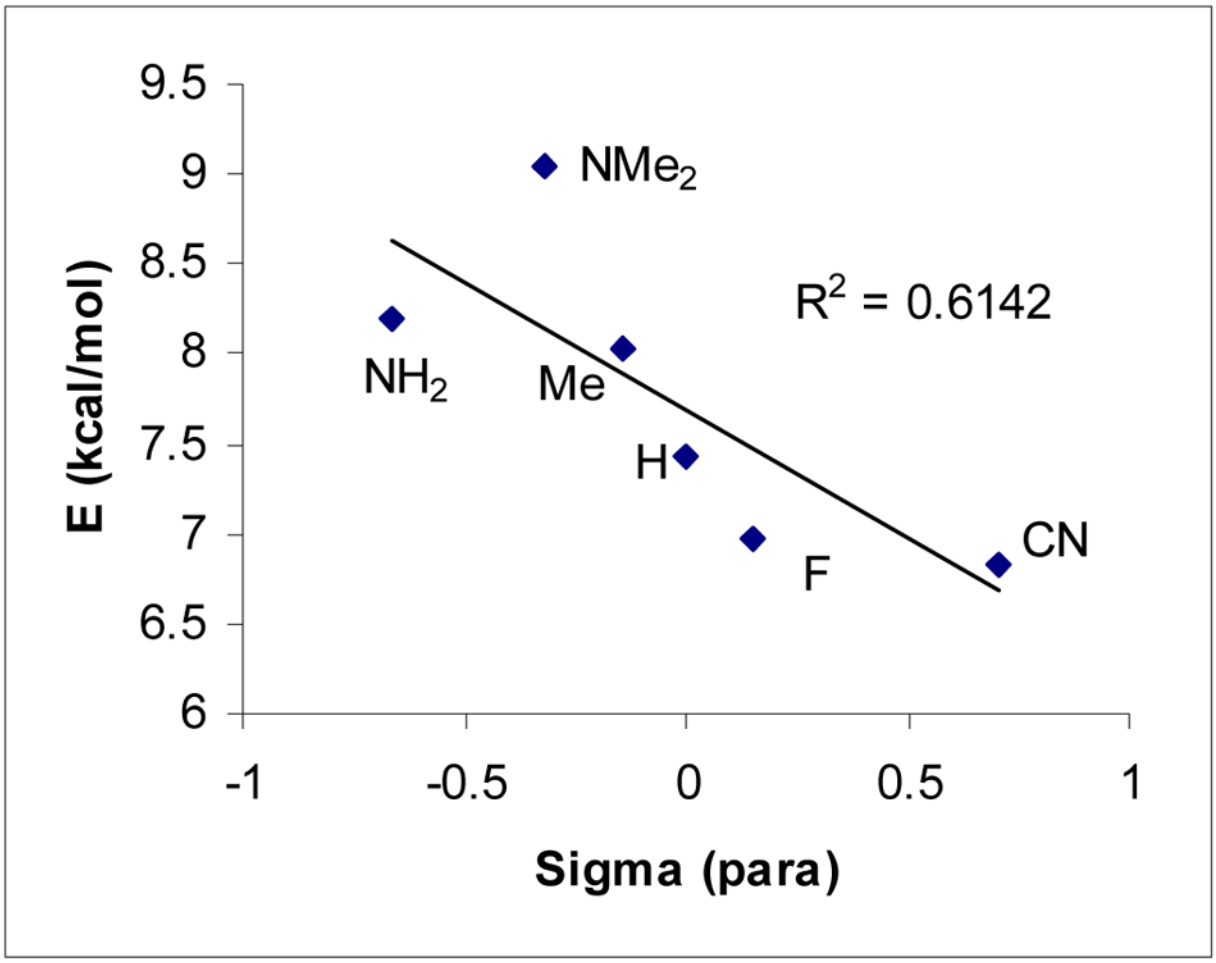

Figure 8.

Plot of binding energy ($-\Delta E_{int}$, MP2(full)/6-31+G**) vs. σ_{para} for complex series **2** C_6F_6-C_6H_5X (♦). Note that the binding energy of C_6F_6-$C_6H_5N(CH_3)_2$ deviates from that predicted by the Hammett parameter by a significant amount, which we suggest is indicative of the presence of charge-transfer interactions.

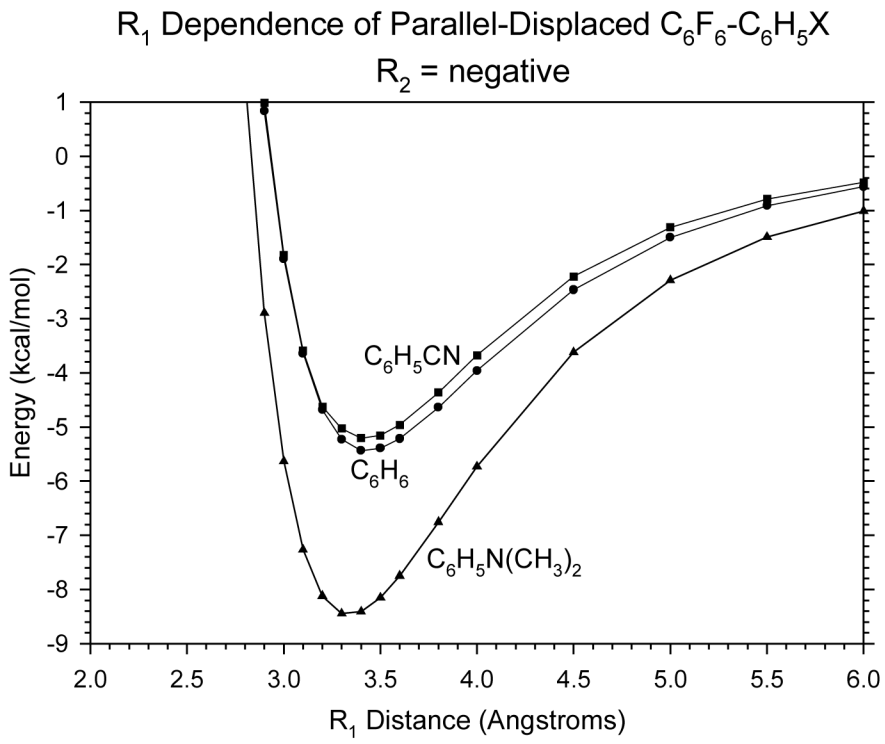

Figure 9.

Plot of interaction energy (MP2(full)/6-31+G**) vs. vertical separation distance for complexes C_6F_6-C_6H_5CN (▪), C_6F_6-C_6H_6 (●), and C_6F_6-$C_6H_5N(CH_3)_2$ (▲). Note that the interaction energy of C_6F_6-$C_6H_5N(CH_3)_2$ is more than 3 kcal/mol larger than the other two complexes at R_1 = 3.3 Å, but levels off to less than 1 kcal/mol when $R_1 \geq 4$ Å. We suggest that the extra attraction at close distance is indicative of the presence of charge-transfer interactions.

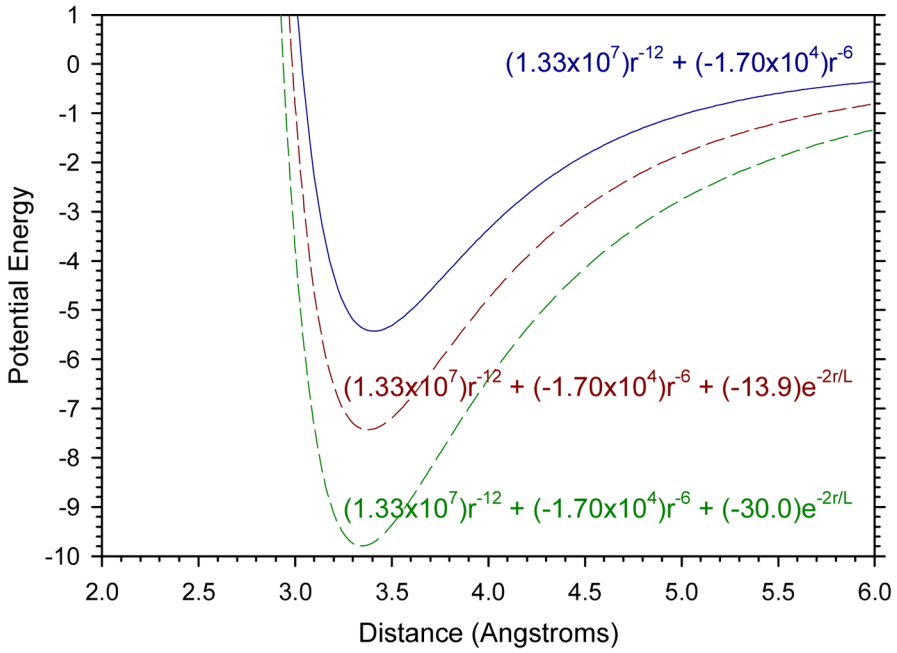

Figure 10.

Potential energy vs. distance plots for (1) Lennard-Jones (—), (2) same as (1) except with an additional charge-transfer term (--), and (3) same as (2) except giving a greater weight to the charge-transfer term (--).

Table 1

Parallel-displaced C_6F_6-C_6H_5X (2a–f) interaction energies (BSSE corrected) at the MP2(full)/6-31+G** optimized R_1 and fixed R_2 = 1.6 Å.

X	CN (a)	F (b)	H (c)	CH_3 (d)	NH_2 (e)	$N(CH_3)_2$ (f)
R_1 (Å)	3.4	3.4	3.4	3.4	3.4	3.4
ΔE_{int} (kcal/mol)	−4.29	−4.60	−4.87	−5.36, −5.43[ab]	−5.79, −5.44[ab]	−6.29, −5.95[ab]

[a] Energy with CH_3 hydrogen, and NH_2 lone pair, and $N(CH_3)_2$ lone pair pointing away from the lower hexafluorobenzene ring.

[b] Energy with CH_3 hydrogen, and NH_2 lone pair, and $N(CH_3)_2$ lone pair pointing towards the lower hexafluorobenzene ring.

Table 2

Parallel-displaced C_6F_6-C_6H_5X (2a–f and 3a–f) MP2(full) BSSE corrected interaction energies (in kcal/mol) at the MP2(full)/6-31+G** optimized R_2 and fixed R_1 = 3.4 Å[a].

X	CN (a)	F (b)	H (c)	CH_3 (d)	NH_2 (e)	$N(CH_3)_2$ (f)
(**2**) Positive R_2(Å)	1.0	1.1	1.0	1.0, 1.0[bc]	1.0, 1.0[bc]	0.9, 0.9[bc]
6-31+G**	−4.83	−5.05	−5.39	−6.12, −6.13[de]	−6.34, −5.88[de]	−7.05, −6.54[de]
6-311+G**	−5.23	−5.42	−5.97	−6.53[d]	−6.73[d]	−7.43, −6.94[de]
6-311++G(2d,2p)	−6.42	−6.57	−7.05	−7.63[d]	−7.82[d]	−8.63, −8.06[de]
aug-cc-pVDZ[f]	−6.82	−6.97	−7.42	−8.02[d]	−8.20[d]	−9.05, −8.46[de]
(**3**) Negative R_2(Å)	−1.3	−1.1	−1.0	−1.0, −0.8[bc]	−0.8, −1.0[bc]	−1.0[g]
6-31+G**	−5.30	−5.41	−5.39	−6.45, −5.55[de]	−6.54, −7.30[de]	−8.41[g]
6-311+G**	−5.77	−5.68	−5.97	−6.90[d]	−7.64[e]	−8.74[g]
6-311++G(2d,2p)	−7.15	−6.90	−7.05	−8.16[d]	−8.77[e]	−10.00
aug-cc-pVDZ[f]	−7.64	−7.34	−7.42	−8.61[d]	−9.19[e]	−10.46[g]

[a] The R_1 = 3.4 Å distance was the optimized distance found when R_2 is fixed at 1.6 Å.

[b] Optimized distance when the CH_3 hydrogen, NH_2 lone pair, and $N(CH_3)_2$ lone pair are pointing away from the lower hexafluorobenzene ring.

[c] Optimized distance when the CH_3 hydrogen, NH_2 lone pair and $N(CH_3)_2$ lone pair are pointing towards the lower hexafluorobenzene ring.

[d] Energy with the CH_3 hydrogen, NH_2 lone pair, and $N(CH_3)_2$ lone pair pointing away from the lower hexafluorobenzene ring.

[e] Energy with the CH_3 hydrogen, NH_2 lone pair, and $N(CH_3)_2$ lone pair pointing towards the lower hexafluorobenzene ring.

[f] Calculations performed at the MP2/aug-cc-pVDZ level.

[g] Optimized distance when the $N(CH_3)_2$ lone pairs is pointing towards the lower hexafluorobenzene ring. A minimum was not found for negative R_2 values with the lone pair pointing away from the lower hexafluorobenzene ring.

Table 3

Sandwich C_6F_6-C_6H_5X (4a–e) interaction energies (BSSE corrected) at the MP2(full)/6-31+G** optimized inter-monomer distances.

X	CN (a)	F (b)	H (c)	CH_3 (d)	NH_2 (e)	$N(CH_3)_2$ (f)
R (Å)	3.6	3.6	3.6	3.5, 3.6[ab]	3.5, 3.6[ab]	3.6, 3.5[ab]
ΔE_{int} (kcal/mol)	−4.41	−4.70	−5.12	−5.78, −5.60[cd]	−6.12, −5.97[cd]	−6.81, −6.91[cd]

[a] Optimized distance when the CH_3 hydrogen, NH_2 lone pair, and $N(CH_3)_2$ lone pair are pointing away from the lower hexafluorobenzene ring.

[b] Optimized distance when the CH_3 hydrogen, NH_2 lone pair, and $N(CH_3)_2$ lone pair are pointing towards the lower hexafluorobenzene ring.

[c] Energy with CH_3 hydrogen, NH_2 lone pair, and $N(CH_3)_2$ lone pair pointing away from the lower hexafluorobenzene ring.

[d] Energy with CH_3 hydrogen, NH_2 lone pair, and $N(CH_3)_2$ lone pair pointing towards the lower hexafluorobenzene ring.